Accessibility of Nitroxide Side Chains: Absolute Heisenberg Exchange Rates from Power Saturation EPR

Christian Altenbach,* Wojciech Froncisz,† Roy Hemker,* Hassane Mchaourab,* and Wayne L. Hubbell*
*Jules Stein Eye Institute and Department of Chemistry and Biochemistry, University of California, Los Angeles, California 90095-7008; and †Department of Biophysics, Faculty of Biotechnology, Jagiellonian University, 30-387 Krakow, Poland

ABSTRACT In site-directed spin labeling, the relative solvent accessibility of spin-labeled side chains is taken to be proportional to the Heisenberg exchange rate (W_{ex}) of the nitroxide with a paramagnetic reagent in solution. In turn, relative values of W_{ex} are determined by continuous wave power saturation methods and expressed as a proportional and dimensionless parameter Π. In the experiments presented here, NiEDDA is characterized as a paramagnetic reagent for solvent accessibility studies, and it is shown that absolute values of W_{ex} can be determined from Π, and that the proportionality constant relating them is independent of the paramagnetic reagent and mobility of the nitroxide. Based on absolute exchange rates, an accessibility factor is defined ($0 < \rho < 1$) that serves as a quantitative measure of side-chain solvent accessibility. The accessibility factors for a nitroxide side chain at 14 different sites in T4 lysozyme are shown to correlate with a structure-based accessibility parameter derived from the crystal structure of the protein. These results provide a useful means for relating crystallographic and site-directed spin labeling data, and hence comparing crystal and solution structures.

INTRODUCTION

SDSL has become a powerful tool for probing structure and dynamics of both water-soluble and membrane proteins of arbitrary molecular weight (1–8). The basic strategy of SDSL involves the substitution of a native residue (or residues) for cysteine, followed by modification of the reactive SH group with a selective nitroxide reagent. The most commonly employed reagent is the methanethiosulfonate derivative that generates the disulfide-linked nitroxide side chain, designated R1 (Fig. 1).

The primary features determined from the EPR spectrum of R1 in a protein are the side-chain motion (9), the Heisenberg exchange rate with paramagnetic reagents in solution (10), and, for proteins containing two paramagnetic centers, the interspin distance (11–14). The Heisenberg exchange rate with suitable paramagnetic reagents has been interpreted in terms of side-chain solvent accessibility, one of the most informative features of the protein fold. For example, the periodic dependence of solvent accessibility with sequence position serves as an independent means of mapping regular secondary structure, and comparison of solvent accessibilities determined by SDSL and computed from crystal structures provide a direct means of comparing solution and crystal structures of a protein (5,15).

Heisenberg exchange between a nitroxide and an ''exchange reagent'' R requires a direct contact interaction in an encounter complex, and the exchange rate, W_{ex}, is taken to be a measure of the exposure of the nitroxide to the solvent containing the reagent. For measurement of solvent accessibility, the reagent should have high water solubility, have limited accessibility to the interior of a well-packed protein, should be electrically neutral, and should be on the order of the size of the nitroxide itself. It is also important that the exchange between the nitroxide and R be in the strong exchange limit, where the rate is determined only by the rate of diffusional encounter and not on details of the encounter complex (16). Finally, it is important that the only manifestation of the reagent/nitroxide interaction is Heisenberg exchange, with little contribution from distance-dependent magnetic dipolar interactions. Otherwise, an interaction could occur through space providing an overestimate of solvent accessibility. This is insured for reagents with $T_{1R} < \tau_c$, where T_{1R} is the longitudinal relaxation time for the reagent and τ_c is the encounter complex lifetime. In this work, it is shown that the complex NiEDDA meets the above criteria as an ideal exchange reagent for determining solvent accessibility.

Heisenberg exchange rates for nitroxide side chains in proteins are most commonly measured using CW power saturation. With some assumptions, the saturation behavior of the nitroxide can be analyzed to provide a widely used ''accessibility parameter'', Π, which is directly proportional to W_{ex} (17,18):

$$\Pi = \alpha W_{ex}.$$

Submitted January 5, 2005, and accepted for publication June 17, 2005.

Address reprint requests to Wayne L. Hubbell, Jules Stein Eye Institute, UCLA School of Medicine, Los Angeles, CA 90095-7008. Tel.: 310-206-8839; Fax: 310-794-2144; E-mail: hubbellw@jsei.ucla.edu.

Hassane Mchaourab's present address is Dept. of Molecular Physiology and Biophysics, Vanderbilt University School of Medicine, Nashville, TN 37232.

Abbreviations used: SDSL, site-directed spin labeling; CW, continuous wave; HE, Heisenberg exchange; NiEDDA, Ni(II)ethylenediaminediacetic acid; T4L, T4 lysozyme; EPR, electron paramagnetic resonance; SR, saturation recovery; 44R1, the mutant with the R1 side chain at site 44 (mutants with a single spin label are given the sequence number for the spin-labeled position followed by R1 designates).

0006-3495/05/09/2103/10 $2.00

doi: 10.1529/biophysj.105.059063

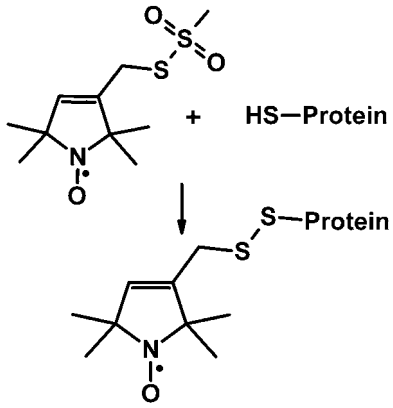

FIGURE 1 The reaction of the spin label with a cysteine to generate the nitroxide side chain R1.

One of the key results of the present study is the determination of the constant α, thus allowing the calculation of absolute exchange rates from experimental values of Π. The values of W_{ex} thus determined for R1 residues in T4L are shown to agree closely with corresponding values measured directly with saturation recovery EPR and reported in a companion paper (19). The correspondence holds for a wide range of spectral lineshapes for R1, thus validating the CW saturation method for determining absolute exchange rate. Collectively, the results are in agreement with the theoretical conclusions of Haas et al. (20) that CW saturation curves should provide a quantitative measure of T_{1e} in nitroxides, even with inhomogeneously broadened lines. Finally, a structure-based measure of R1 solvent accessibility in proteins is introduced that correlates with W_{ex} and a related accessibility factor (ρ) for both NiEDDA and oxygen as exchange reagents.

MATERIALS AND METHODS

T4L mutants and EPR spectroscopy

T4 lysozyme mutants containing the R1 side chain were previously reported (21). NiEDDA was synthesized according to Oh et al. (18). EPR spectra were recorded on a Varian E-109 spectrometer fitted with a two-loop-one-gap resonator (22) over a field range of 100 G. Samples were contained in gas permeable TPX capillaries and equilibrated with either air for Heisenberg exchange measurements with oxygen, or equilibrated with nitrogen in all other cases. For CW power saturation measurements, the central line was recorded as a function of microwave power and the peak to peak first derivative amplitude analyzed as described to obtain the accessibility parameter Π (18).

To measure the Lorentzian line broadening in EPR spectra, the broadened first-derivative spectrum was fitted as a convolution of the first-derivative spectrum in the absence of R and a Lorentzian broadening function, using a Levenberg Marquardt fitting procedure written in LabVIEW (National Instruments, Austin, TX). The three adjustable parameters were the: 1), Lorentzian width at half-height ($\Delta H_{1/2}$); 2), field position offset; and 3), area of the Lorentzian. Because the two spectra are well aligned and contain a similar number of spins, the position offset was always close to zero and the area close to 1 as expected. The best fit width is directly related to the additional broadening caused by Heisenberg exchange according to $W_{ex} = 0.5\gamma\Delta H_{1/2}$ (see below). A similar method was used by Smirnov et al. (23) to measure oxygen broadening. In this case, measurements in the absence and presence of oxygen can be done on the same sample under identical settings with only $dH_{1/2}$ as an adjustable parameter. In the case of NiEDDA, two different samples are required and the additional area and shift parameters are required to account for small dilution and field offsets errors.

Estimation of nitroxide side-chain solvent accessibility from a crystal structure

The fractional solvent-exposed surface area (f_{SA}) for the native amino acid at each sequence position was calculated from the crystal structure using the program Molmol (24). A structure-based accessibility parameter f_V (fractional volume) characteristic of a given site without the side chain, was calculated from the crystal structure using InsightII software (Accelrys, San Diego, CA). First, the amino acid was replaced by glycine. A spherical volume centered at the α-carbon with radius 8 Å was filled with water, and all water molecules that overlap with the protein structure removed. The number of remaining water molecules was divided by their original count, yielding an estimate of the free fractional volume near the site of interest that is potentially accessible to the R1 side chain.

THEORY

Heisenberg exchange rates and nitroxide side-chain accessibility

For a bimolecular encounter between a small nitroxide (N) in solution and an exchange reagent R, the Heisenberg exchange frequency, W_{ex}, experienced by a particular nitroxide is given by

$$W_{ex} = k_{ex}C_R, \quad (1)$$

where k_{ex} is the exchange rate constant and C_R is the concentration of R. In the strong exchange limit, where Heisenberg exchange is diffusion controlled, k_{ex} is given by (cgs units)

$$k_{ex} = P_{max} f\, k_D = P_{max} f\, 4\,\pi(N_A/1000)(D_N + D_R)\, r_c, \quad (2)$$

where P_{max} is the maximum exchange efficiency, f is the ''steric factor'', $k_D = 4\pi(N_A/1000)\ (D_N + D_R)\ r_c$ is the diffusion-controlled rate constant, and D_N and D_R are the diffusion constants for the nitroxide and reagent, respectively. The collision radius, r_c, is $r_N + r_R$, where r_N and r_R are the effective radii of the nitroxide and reagent, respectively. The dimensionless steric factor is necessary to account for exchange between molecules where particular relative orientations are required for exchange. When the encounters are in the strong exchange limit and $T_{1R} < \tau_c$, $P_{max} = 1$ (16). This is apparently the case for O_2 (25) and, as discussed below, for NiEDDA.

For a nitroxide tethered to a protein, it is assumed that the nitroxide translational diffusion coefficient becomes that of the protein itself, comparatively very small, and thus $D_N + D_R \approx D_R$. However, the nitroxide retains rotational degrees of freedom about the bonds of the tether. The definition of the collision radius, r_c, is retained, because R and the nitroxide (rather than the protein to which it is attached) are still viewed as the colliding species. The local protein

environment, and interactions of the nitroxide with the protein, may reduce the number of effective collisions below that characteristic of the nitroxide in solution, and all such effects are collectively accounted for by a factor ρ, the ''accessibility factor''. Thus, for a protein-associated nitroxide, W_{ex}^{P} in the strong exchange limit is

$$W_{ex}^{P} = \rho f\, 4\,\pi (N_A/1000)\, D_R\, r_c\, C_R. \quad (3)$$

For a small, electrically neutral but polar exchange reagent, ρ varies from 0 for a nitroxide buried in the protein interior to a limiting value of unity for a nitroxide at a completely exposed site on the protein surface. With Eqs. 1 and 3, ρ can be expressed as the ratio of the exchange rate constant for the nitroxide in the protein to that in solution, scaled by a ratio of diffusion constants:

$$\rho = k_{ex}^{P}/k_{ex}[(D_R + D_N)/D_R], \quad (4)$$

where $k_{ex}^{P} = W_{ex}^{P}/C_R^{P}$, $k_{ex} = W_{ex}/C_R$, and C_R^{P} and C_R are the concentrations of R at which the corresponding exchange rates apply. As discussed below, Eq. 4 may be employed together with experimental values of exchange rates and relative values of D_R and D_N to determine ρ for a nitroxide at any site.

Measurement of Heisenberg exchange rate

In general, for exchange reagents with $T_{1R} < \tau_c$, T_{1e} Heisenberg exchange leads to equal changes in T_{1e} and T_{2e} of the nitroxide, and

$$W_{ex} = \Delta[1/T_{1e}] = \Delta[1/T_{2e}] = k_{ex}C_R. \quad (5)$$

Thus, methods based on measurement of either T_{2e} or T_{1e} may be employed for experimental determination of W_{ex}. Methods based on T_{2e} rely on the fact that Heisenberg exchange leads to Lorentzian line broadening. As described in Materials and Methods, the broadening can be determined as the width at half height of the Lorentzian line ($\Delta H_{1/2}$) that, when convoluted with the spectrum in the absence of collision, yields the interacting spectrum. Alternatively the broadening can be directly measured as the increase in peak-to-peak central linewidth of the first derivative EPR spectrum ($\Delta\Delta H_{pp}$). Note that $\Delta H_{1/2} = 3^{1/2}\Delta\Delta H_{pp}$. W_{ex} is obtained from either method according to:

$$\begin{aligned} W_{ex} &= \Delta[1/T_{2e}] = \gamma\Delta H_{1/2}/2 = 0.44\times 10^{7}\,(\mathrm{g})\,\Delta H_{1/2} \\ &= 0.44\times 107\,(g)\,3^{1/2}\Delta\Delta H_{pp}, \end{aligned} \quad (6)$$

where g is the g factor of the nitroxide. Simplicity of measurement and direct determination of absolute exchange frequency are the advantages of this approach. In the experiments presented below, $\Delta H_{1/2}$ determined by convolution and $\Delta\Delta H_{pp}$ are both employed to measure W_{ex}. In general, the convolution approach is more accurate, especially for noisy spectra and small broadening, because the entire lineshape is used to obtain the result. Determination of $\Delta\Delta H_{pp}$ requires two independent ΔH_{pp} measurements, each relatively inaccurate in the usual case of significant spectral noise.

Two T_{1e}-based methods for measurement of W_{ex} due to fast-relaxing exchange reagents are in common use: CW saturation and saturation recovery. SR provides a direct determination of the nitroxide T_{1e}, and is the subject of a companion paper (19). For CW saturation, the amplitude (A) of the first derivative central ($m_I = 0$) resonance line is measured as a function of microwave power (P), and the data fit to the function

$$A = I\,P^{1/2}[1 + (2^{1/\varepsilon} - 1)P/P_{1/2}]^{-\varepsilon}, \quad (7)$$

with I, $P_{1/2}$, and ε as adjustable parameters. This function describes the saturation of a first derivative EPR signal of arbitrary homogeneity (18). Parameter I is a scaling factor, $P_{1/2}$ is the incident microwave power where the first derivative amplitude is reduced to half of its unsaturated value, and ε is a measure of homogeneity of the saturation. For the homogeneous and inhomogeneous saturation limits, $\varepsilon = 1.5$ and 0.5, respectively. Generally, the saturation of the R1 side chain in proteins in the absence of collision reagent is found to be homogeneous as judged by ε. For a homogeneous Lorentzian,

$$P_{1/2} = (2^{2/3} - 1)/(\Lambda^2\gamma^2 T_{1e}T_{2e}), \quad (8)$$

where $\Lambda = H_1/P^{1/2}$ is the resonator efficiency (26) and $\gamma = g\beta 2\pi/h$. For the common case where $W_{ex} \ll 1/T_{2e}$, T_{2e} may be taken as a constant, and

$$\begin{aligned} \Delta P_{1/2} &= P_{1/2} - P_{1/2}^{o} = (2^{2/3} - 1)/(\Lambda^2\gamma^2)1/T_{2e}[1/T_{1e} - 1/T_{1e}^{o}] \\ &= ((2^{2/3} - 1)/(\Lambda^2\gamma^2 T_{2e}))(W_{ex}), \end{aligned} \quad (9)$$

where $P_{1/2}$ and $P_{1/2}^{o}$ are in the presence and absence of R, respectively, and T_{1e} and T_{1e}^{o} are the corresponding relaxation times. Although $\Delta P_{1/2}$ is proportional to W_{ex}, it depends on the motion of the nitroxide through T_{2e} and on properties of the resonator through Λ. To reduce or eliminate these dependencies, the dimensionless quantity Π was defined (17,18) as

$$\Pi = [\Delta P_{1/2}/\Delta H_{pp}]/[P_{1/2}/\Delta H_{pp}]_{reference} = \alpha W_{ex}. \quad (10)$$

Division of $\Delta P_{1/2}$ by the nitroxide central linewidth, ΔH_{pp}, normalizes for the nitroxide T_{2e}, and division by the quantity $[P_{1/2}/\Delta H]_{reference}$ normalizes for variations in resonator efficiency. In published literature to date, a dilute DPPH powder in KCl was selected as the reference, and the reported Π values depend on this choice. In this study, α was determined using Eqs. 6 and 10 and a comparison of data from line broadening with that from CW saturation for R1 at a solvent exposed site in T4L. Values of W_{ex} calculated from experimental values of Π and α are shown to agree well with those determined from SR reported in a companion article (19).

RESULTS

NiEDDA-nitroxide encounters in solution

To be useful in estimating nitroxide solvent accessibility, a nitroxide-exchange reagent encounter should be in the strong exchange (diffusion-controlled) limit. To examine this point for NiEDDA, the exchange rate with a small nitroxide in solution was investigated as a function of solution viscosity. According to Eqs. 1 and 2, the exchange rate is given by

$$W_{ex} = f\,k_D\,C_R = f\,4\,\pi(N_A/1000)(D_N + D_R)r_c\,C_R = [f\,kTN_A/750][r_N + r_R]^2/[r_N\,r_R]C_R/\eta, \quad (11)$$

where the substitutions $D = kT/6\pi\eta r$, $r_c = r_N + r_R$ have been made, and k is the Boltzmann constant. Thus, in the strong exchange limit, W_{ex} is a linear function of $1/\eta$. Fig. 2 shows a plot of experimental values of W_{ex} vs. $1/\eta$ for the small nitroxide 4-cyano-2,2,5,5-tetramethylpryollidine-1-oxyl in the presence of NiEDDA at a fixed concentration of 3 mM. In this case, line broadening was measured as $\Delta\Delta H_{pp}$ and W_{ex} computed from Eq. 6. The linearity of the plot confirms that exchange is diffusion controlled, i.e., in the strong exchange limit. In addition, $\Delta\Delta H_{pp} \rightarrow 0$ as $1/\eta \rightarrow 0$ ($\eta \rightarrow \infty$), showing that there is no dipolar contribution to the line broadening. This result implies that $T_{1R} < \tau_c$ for NiEDDA, supporting the assignment of $P_{max} = 1$ (see Eq. 2 and related discussion).

Fig. 3 *A* shows the EPR spectra of 4-cyano-2,2,5,5-tetramethylpryollidine-1-oxyl in aqueous solution at a fixed viscosity ($\eta = 1$ cP) as a function of NiEDDA concentration (*gray trace*). In this study, line broadening was determined by the Lorentzian convolution method. The Lorentzian used to obtain the best fit to the experimental spectrum is shown superimposed on the data, along with the best-fit spectrum (*black trace*). W_{ex} was computed from the width of the Lorentzian ($\Delta H_{1/2}$) and Eq. 6, and plotted as a function of concentration in Fig. 3 *B*. As predicted for the strong exchange limit by Eq. 11, the relationship is linear with a slope of 1.21 ± 0.02 MHz/mM, the exchange rate constant for the nitroxide-NiEDDA encounter.

The steric factor, f, for the NiEDDA-nitroxide encounter may now be estimated from Eq. 2 as $f = k_{ex}/k_D$. From the definition of the diffusion-controlled exchange constant k_D,

$$k_D = 4\pi(N_A/1000)(D_N + D_R)(r_N + r_R) = (RT/1500\eta)(r_N + r_R)^2/r_N r_R, \quad (12)$$

where the substitution $D = kT/6\pi\eta r$ has been made for the two diffusion constants, assuming that the encounter partners can be approximated as spherical in shape. For a nitroxide and reagent of the same size, $(r_N + r_R)^2/r_N r_R = 4$, and

$$k_D = 4RT/1500\eta. \quad (13)$$

This remarkable result shows that the diffusion-controlled rate constant is independent of size, as long as the two species are the same size. To a good approximation, Eq. 13 holds for reagents and nitroxides of similar size. For example, if one radius is off by a factor of two, the error incurred is only ~10%. Thus, Eq. 13 should apply reasonably well for NiEDDA (mol wt = 232) and a nitroxide such as 4-cyano-2,2,5,5-tetramethylpryollidine-1-oxyl (mol wt = 165), avoiding the necessity of estimating the hydrodynamic radii of the species involved. According to Eq. 13, $k_D \approx 6.5$ Mhz/mM, Thus, the steric factor, $f = k_{ex}/k_D \approx 0.20$.

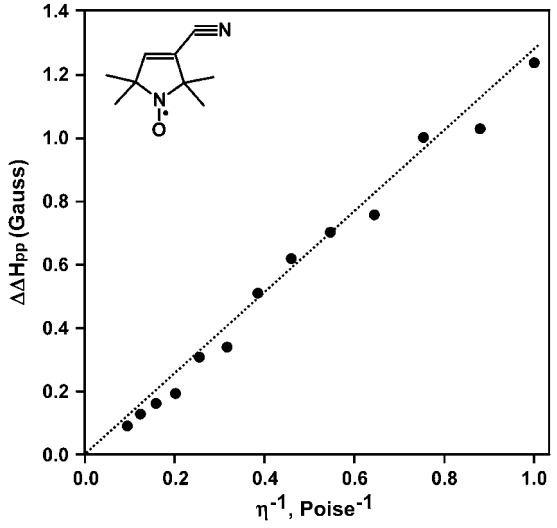

FIGURE 2 Line broadening of 4-cyano-2,2,5,5-tetramethylpryollidine-1-oxyl in solution by 3 mM NiEDDA as a function of viscosity. Line broadening at constant ambient temperature was measured directly as $\Delta\Delta H_{pp}$ from the first-derivative EPR spectra, and viscosity was varied by addition of glycerol.

NiEDDA and O_2 encounters with the R1 side chain in T4L

Fig. 4 shows the locations of the T4L sites investigated in this study. Residues 128–135 lie in a short α-helix (two turns), where the side chains span the full range of solvent accessibility, from completely buried to solvent exposed. These are the same sites investigated by SR in a companion article (19). Other sites were selected to represent additional solvent-exposed helix surface sites (residues 44, 65, 72), a partially solvent-exposed site (residue 74), and C-terminal helix sites (residues 81, 89). The EPR spectra for R1 at each of the sites in Fig. 4 are shown in Fig. 5 for T4L in buffer. Spectra for R1 at these sites have been previously published (21), but in that study they were recorded in 30% sucrose to reduce the rotational diffusion of the protein. Even with a contribution from protein rotation present, it is easy to identify the buried sites 129 and 133 by the broad spectral line shapes corresponding to slow motion. Collision studies should preferably be done without sucrose, because it would reduce the translational diffusion of the agents, lowering the observed collision rate.

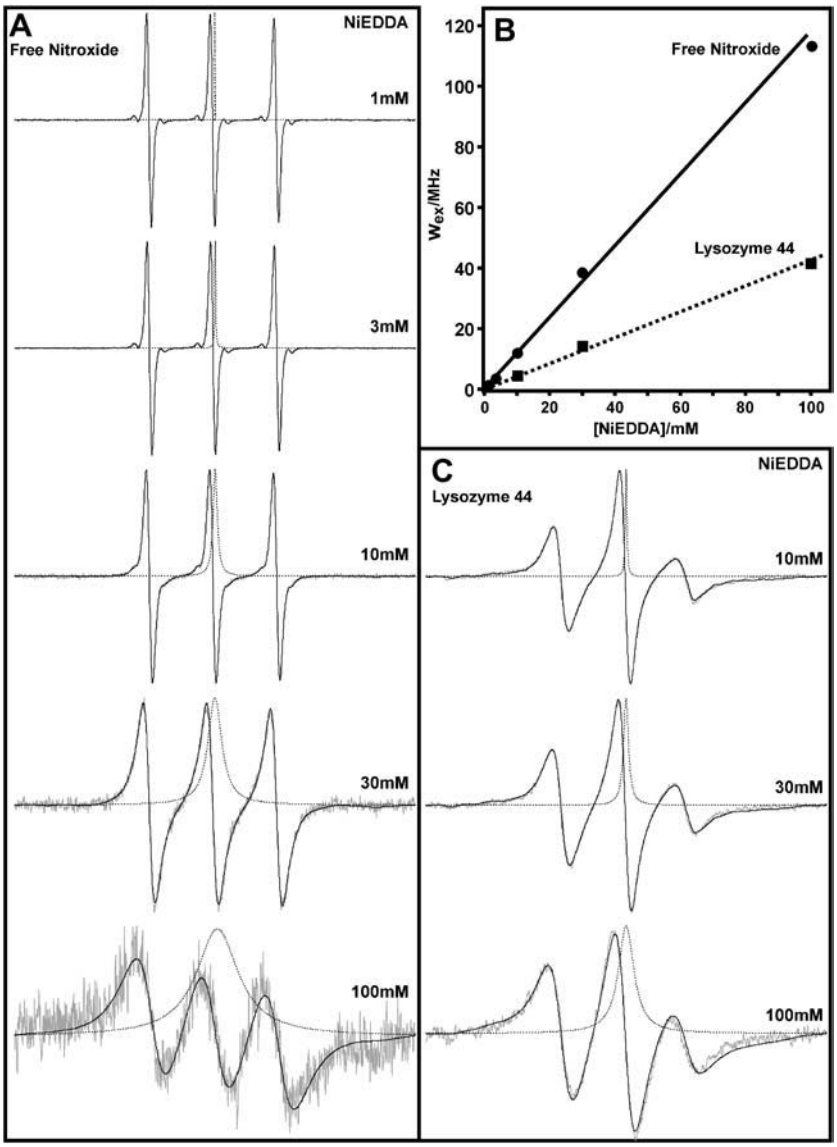

FIGURE 3 (*A*) Lorentzian broadening of 4-cyano-2,2,5,5-tetramethylpryollidine-1-oxyl due to Heisenberg exchange at different concentrations of NiEDDA. The EPR spectrum is shown in gray. Each spectrum was fitted to a convolution of the spectrum in the absence of NiEDDA and a single Lorentzian line as described in Materials and Methods. The best fit is shown in black and the corresponding Lorentzian as a dotted line. (*B*) The exchange frequency is calculated directly from the best-fit Lorentzian in panels *A* and *C*, and plotted versus the concentration of NiEDDA. (*C*) Lorentzian broadening of T4L 44R1 due to NiEDDA. The EPR spectrum is shown in gray. Each spectrum was fitted to a convolution of the spectrum in the absence of NiEDDA and a single Lorentzian line as described in Materials and Methods. The best fit is shown in black and the corresponding Lorentzian as a dotted line.

For each of these sites, Π was determined for NiEDDA at 3 mM and for O_2 at ~0.27 mM, the concentration in buffer at equilibrium with air. The values are given in the first two columns of Table 1, normalized by the concentration of reagent ($k_{ex} = \Pi/C_R$). At all sites, $k_{ex}(O_2)$ is significantly greater than k_{ex}(NiEDDA), due in part to the larger diffusion coefficient of O_2. In previous work, native residues have been classified as ''solvent accessible'', ''partially solvent accessible'', or ''buried'' based on the fractional solvent accessibility (f_{sa}) computed from the crystal structure by the method of Lee and Richards (15). The fractional solvent accessibility for the native residue at each site is also given in Table 1. For R1 at solvent-accessible sites ($f_{sa} > 0.25$) the ratio $k_{ex}(O_2)$ / k_{ex}(NiEDDA) is roughly constant (Table 1, column 3). However, for R1 at partially solvent-accessible ($0.05 < f_{sa} < 0.25$) or buried ($f_{sa} < 0.05$) sites, the ratio increases dramatically.

For R1 at the solvent-exposed sites 44 and 65 and at the partially solvent-exposed site 74, Π was determined as a function of NiEDDA concentration. As shown in Fig. 6, the relationship is linear and the slopes, which reflect the relative solvent accessibilities of the R1 side chain, are 0.24, 0.17, and 0.04 mM^{-1}, respectively (corresponding to the values for k_{ex} in Table 1). NiEDDA concentrations above ~10 mM could not be used in Π determination of 44R1 and 65R1 because of line broadening effects, which were not apparent up to 30 mM in the less accessible 74R1.

The R1 side chain at the solvent-accessible position 44 in T4L was selected as an ideal site for comparison of Π and W_{ex}^{P} and for determination of the proportionality constant α of Eq. 10. Because of the high accessibility (Table 1; Fig. 6) and relatively narrow linewidth (Fig. 5) of R1 at this site, measurable line broadening was produced by NiEDDA in the range of 10–100 mM, providing an absolute determination

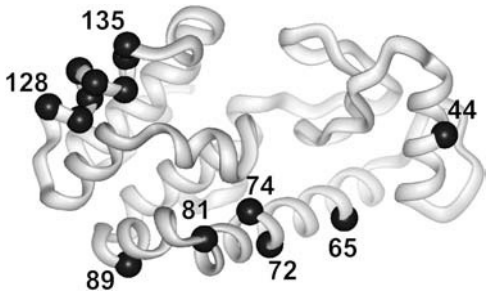

FIGURE 4 Ribbon model of T4L showing the location of the sites investigated as spheres on the corresponding α-carbon.

of W_{ex}^{P} via Eq. 6. Fig. 3 *C* shows the NiEDDA-induced Lorentzian line broadening for 44R1 analogous to the experiment with the free nitroxide shown in Fig. 3 *A*. Fig. 3 *B* shows the derived W_{ex}^{P} as a function of NiEDDA concentration. The exchange rate constant determined from the slope is 0.44 $\pm$ 0.02 MHz/mM for 44R1 over the concentration range 10–100 mM. Two factors contribute to the lower value compared to the result with the free nitroxide ($k_{ex} = 1.21$ MHz/mM). The translational diffusion rate of the spin label attached to the protein is negligible compared to the free label, while the NiEDDA diffusion is the same. Because NiEDDA and the nitroxide are of similar size this will cause an ~50% reduction in collision rate. The remainder of the difference is due to the presence of the protein structure. Accounting for the diffusion effect, the presence of the protein causes only a 30% reduction in collisions for such an exposed site.

The slope of the W_{ex}^{P} versus NiEDDA concentration plot in Fig. 3 *B* and that for the Π versus NiEDDA plot in Fig. 6 determine the important constant $\alpha = W_{ex}/\Pi = 0.44/0.24 = 1.8 \pm 0.1$ MHz. With this value Π data can now be expressed directly in terms of absolute exchange rate according to W_{ex} (MHz) $= 1.8\Pi$, or as the concentration-independent rate constant $k_{ex}^{P} = 1.8\Pi/C_{R}^{P}$, the latter of which could be taken as a quantitative experimental measure of solvent accessibility for R1 in a protein.

An alternative to k_{ex}^{P} as a measure of accessibility is the more intuitive ''accessibility factor'' ρ given by Eq. 4. The accessibility factor ranges from 0 for a buried site to 1 for a nitroxide with accessibility equal to that of a free nitroxide in solution. To estimate the accessibility factor for any site using experimental values of k_{ex}^{P} and Eq. 4, the quantities $[(D_N + D_R)/D_R]$ and k_{ex} are required, where D_N and k_{ex} refer to the small ''reference'' nitroxide 4-cyano-2,2,5,5-tetramethylpryollidine-1-oxyl in solution. Because of the similar size of the reference nitroxide and NiEDDA, $[(D_N + D_R)/D_R] \approx 2$, a choice supported by diffusion coefficients computed from the Wilke-Chang equation and molar volumes of the compounds (27). Using $k_{ex} = 1.2$ MHz/mM appropriate for the encounter of NiEDDA and the reference nitroxide, and $\alpha = 1.8$ MHz/mM to convert to Π values, Eq. 4 gives

$$\rho(\text{NiEDDA}) \approx 1.67[k_{ex}^{P}] \approx 3\Pi/C_{R}^{P}. \quad (14)$$

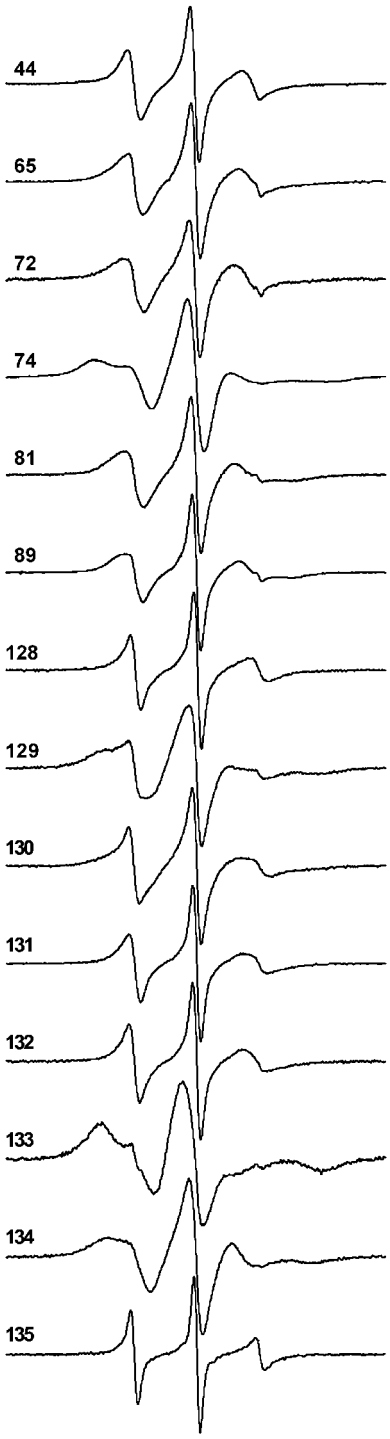

FIGURE 5 EPR spectra of T4L mutants containing the R1 nitroxide side chain at the designated position. All spectra are recorded in buffer at ambient temperature.

Clearly the value of ρ given in Eq. 14 depends on the choice of exchange reagent, and it is thus designated. Values for ρ(NiEDDA) for all residues investigated are given in Table 1, and will be discussed further below for particular cases.

TABLE 1 Parameters characterizing Heisenberg exchange rates for R1 in T4L

Residue	k_{ex}(NiEDDA)*	$k_{ex}(O_2)$	$k_{ex}(O_2)/k_{ex}$(NiEDDA)	$f_{sa}^{\dagger}$	$f_V^{\ddagger}$	ρ
44	0.213	1.89	8.85	0.80	0.42	0.64
65	0.173	1.52	8.76	0.74	0.36	0.52
72	0.140	1.67	11.90	0.55	0.38	0.42
74	0.040	0.70	17.59	0.10	0.07	0.12
81	0.197	1.59	8.10	0.17	0.18	0.59
89	0.290	2.00	6.90	0.57	0.41	0.87
128	0.290	2.00	6.90	0.55	0.49	0.87
129	0.037	0.70	19.19	0.00	0.10	0.11
130	0.173	1.44	8.33	0.12	0.15	0.52
131	0.233	2.07	8.89	0.68	0.44	0.70
132	0.300	1.78	5.93	0.31	0.27	0.90
133	0.003	0.19	55.56	0.01	0.06	0.01
134	0.147	1.52	10.35	0.30	0.22	0.44
135	0.333	2.04	6.11	0.80	0.44	1.00

*$k_{ex} = \Pi/C_R$, where C_R is the concentration of reagent corresponding to Π.
†f_{sa} is the fractional surface area accessibility of the native side chain calculated according to Lee and Richards (31).
‡f_V is the fractional volume accessibility computed as described in Materials and Methods.

The constant α relating W_{ex} and Π should be independent of the nature of the exchange reagent, as long as $T_{1R} < T_{1e}$, and independent of the EPR spectral lineshape (mobility). In principle, this could be checked by determining α using the method described above at sites other than 44, representing the full range of motion, and with other exchange reagents. However, line broadening due to exchange is only measurable at highly exposed, and therefore mobile, sites. As an alternative approach, absolute values of W_{ex}^P for both NiEDDA and O_2 derived from CW power saturation were compared to those from SR, which measures W_{ex}^P directly. Moreover, data were compared for R1 residues at eight sequential positions along an α-helical sequence in T4L (residues 128–135) where the nitroxide mobility and lineshape varied widely. Fig. 7 *A* summarizes the data as a function of sequence position. As is evident, W_{ex}^P derived from both methods and for both exchange reagents reveals the periodicity of the α-helix. For comparison, Fig. 7 *A* also shows ρ(NiEDDA) determined from CW saturation; as expected, it varies from 0 to 1. Of particular interest is the striking agreement between the absolute values of W_{ex}^P derived from CW saturation and SR methods for both reagents for all sites. This similarity is emphasized in the plot of Fig. 7 *B* that directly compares the values from the two techniques. The dashed trace is the ideal case with a slope = 1. The excellent agreement suggests that the constant α is independent of the location or mobility of the nitroxide in the protein, from highly mobile exposed sites to essentially immobilized buried sites, and independent of the exchange reagent.

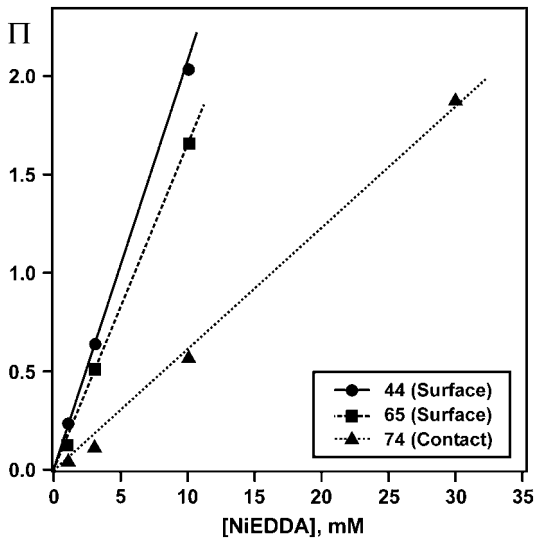

FIGURE 6 The accessibility parameter Π versus concentration of NiEDDA for residues 44R1, 65R1, and 74R1.

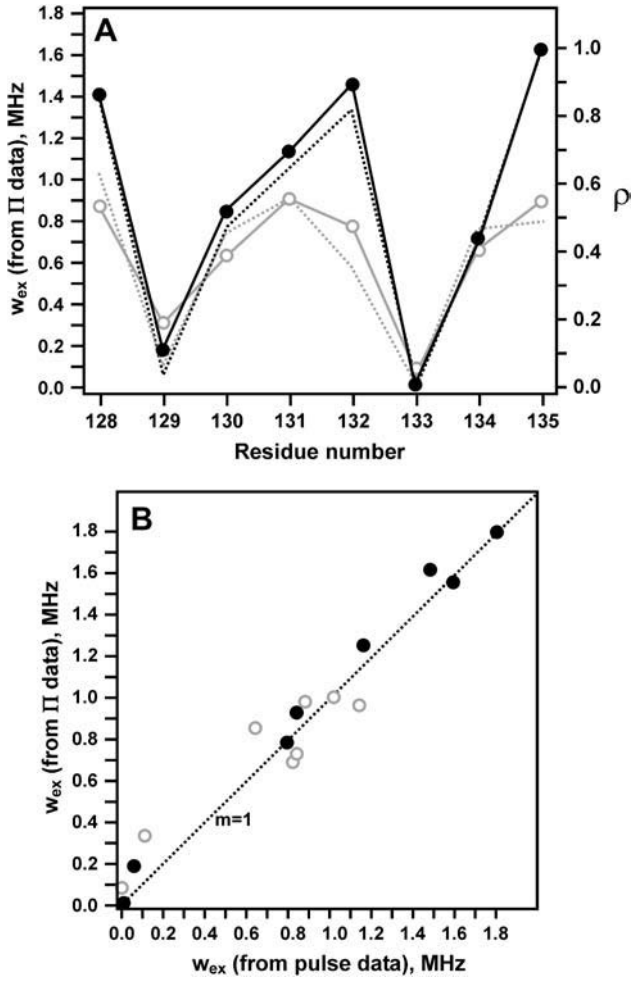

FIGURE 7 Correlation of W_{ex} determined by CW saturation and by saturation recovery EPR. (*A*) W_{ex} for NiEDDA (*black*) and O_2 (*gray*) determined by SR and CW saturation are plotted for R1 residues along the sequence 128–135. SR data is taken from Pyka et al. (19) and shown as dotted lines with the same color scheme. The right axis shows the same data in units of ρ. (*B*) W_{ex} determined from SR is plotted versus W_{ex} from CW saturation. Open gray circles are data for O_2, and solid circles for NiEDDA. The dashed line has a slope of 1, passing through the origin.

Relation of ρ(NiEDDA) to solvent accessibility computed from the crystal structure

The data presented above suggest that ρ(NiEDDA) may be a reasonable experimental measure of the solvent accessibility of the R1 side chain in proteins. To examine this idea, a measure of the exposure of the side chain accessible to solvent is required. As a first approximation, the solvent-accessible surface area of the original native side chain (f_{SA}) computed from the crystal structure might be employed. This approach was used to compare Π values with the solvent-accessible surface areas of rhodopsin (5) and annexin (15). Although a good correlation was found for many sites, native residues that had significantly different size compared to R1, and residues that were involved in specific interactions were problematic. For the sites in T4L studied here, the correlation of f_{SA} and ρ(NiEDDA) is poor (correlation coefficient 0.69; data not shown). A refinement would be to replace the native amino acid with an energy minimized R1 side chain, and compute the solvent accessible from the model. Unfortunately, the true conformation of the R1 side chain at the various sites is not known, and the measure must be based on properties of the environment around the site in question. For one such measure the native side chain is removed and replaced with a glycine. A sphere of radius 8 Å (approximate size of the R1 side chain) is drawn centered on Cα, and a parameter f_V is calculated as the fraction of the available spherical volume filled with water, as described in Materials and Methods. The maximum value of f_V for residues on helical surfaces is $\approx$0.5, because roughly half of the sphere contains backbone atoms. Fig. 8 shows a plot of W_{ex} (NiEDDA) and $W_{ex}(O_2)$ versus f_V for all sites investigated. As is apparent, the parameters are well correlated over the full range of sites investigated here.

DISCUSSION

NiEDDA and oxygen as exchange reagents

Both NiEDDA and O_2 have been extensively used as paramagnetic reagents to determine nitroxide side-chain solvent accessibility, but NiEDDA has not been previously characterized with respect to exchange parameters. As shown in Fig. 2, the NiEDDA-nitroxide exchange rate in glycerol-water mixtures is proportional to η^{-1}, demonstrating a diffusion-limited mechanism consistent with a strong exchange interaction ($J\tau_C > 1$, where J is the exchange integral). Importantly, the line broadening becomes undetectable at high viscosity ($\Delta\Delta H_{pp} \rightarrow 0$ as $\eta^{-1} \rightarrow 0$), showing that there is little linewidth contribution from magnetic dipolar interaction between NiEDDA and the nitroxide (16). This suggests that the spin-lattice relaxation time of NiEDDA is short compared with the lifetime of the encounter complex, a circumstance that leads to high collision efficiency (16). The diffusion-controlled rate constant for exchange between NiEDDA and the small nitroxide 4-cyano-2,2,5,5-tetramethylpryollidine-1-oxyl was determined to be 1.21 $\pm$ .02 MHz/mM (1.21×10^9 $M^{-1}s^{-1}$), similar to that found for other Ni(II) complexes in aqueous solution (28). Together with the high water solubility (>200 mM) and inaccessibility to the interior of proteins (Table 1; Fig. 7 *A*), these properties make NiEDDA an excellent choice as a probe for solvent accessibility of nitroxide side chains in soluble proteins.

Oxygen is a very convenient reagent for accessibility measurements, because it can be readily added and removed through the use of gas permeable capillaries as EPR sample containers. The exchange rate constant for O_2 with small nitroxides in solution is 8.1 $\pm$ 0.2 MHz/mM (23), significantly larger than that for NiEDDA, and O_2 has a size more similar to H_2O than does Ni(EDDA). However, the actual concentration of oxygen in water equilibrated with a gas mixture depends on many experimental variables, such as temperature, partial pressure of oxygen, and buffer composition (29). For example, a change in temperature from 25 to 15° will cause an ~20% increase in oxygen concentration.

Table 1 shows that the ratio $k_{ex}(O_2)/k_{ex}$(NiEDDA) (and the corresponding ratio of exchange rates) is relatively constant for exposed residues ($f_{SA} > 0.25$), even though the individual values vary by more than a factor of 2. Thus, $W_{ex}(O_2)$ and W_{ex}(NiEDDA) are equivalent measures of solvent accessibility in this regime. However, for partially solvent-exposed and buried residues ($f_{SA} < 0.25$) there is a dramatic decrease in the accessibility of NiEDDA relative to O_2. This ''steric exclusion'' effect has been previously noted (15), and is likely due to differential penetration of the relatively small and nonpolar O_2 into the protein interior. Thus, NiEDDA has a higher contrast for mapping solvent accessibility. For the above reasons, NiEDDA is the preferred probe for determination of ρ.

Experimental measures of Heisenberg exchange

Here and in a companion article (19), three methods for measurements of Heisenberg exchange rates have been employed: SR, spectral line broadening, and CW power saturation. Each has strengths and weaknesses depending on the application. For example, in the presence of multiple spin populations SR has an advantage because it can resolve multiple components and identify differential accessibility in the presence of exchange reagents (19). CW power saturation cannot easily distinguish between two homogenously saturating components with different accessibility and a single component with inhomogeneous saturation. Direct measurement of line broadening in the presence of multiple spectral components is also difficult to analyze; direct $\Delta\Delta H_{pp}$ measurements will favor the sharpest component, which could be a minority component, and the simple convolution approach for measurement of $\Delta H_{1/2}$ is not possible if two components show differential broadening.

Because $T_1 \gg T_2$ for R1 in proteins, the T_1-based methods of CW power saturation and SR can detect much lower

exchange rates than the T_2-based line broadening methods; in general, line broadening is not attractive for characterizing partially solvent accessible sites in proteins. However, line broadening and SR have a distinct advantage in that they provide absolute values of exchange rates, while CW saturation only provides parameters such as Π that are proportional to exchange rates through a reference-dependent constant. Moreover, a number of assumptions underlie the apparent proportionality. Because of the simplicity and wide availability of the CW saturation method compared to SR, it is desirable to validate the method and determine strategies for evaluating the proportionality constant so that absolute exchange rates can be reported. In this work, the proportionality constant, α, between Π and W_{ex} was determined by comparing line broadening and CW saturation results for a reference sample (T4L 44R1) where data could be collected for both methods in the same concentration range of exchange reagent. The value of α thus determined depends on the choice of reference used in the saturation studies; DPPH powder in KCL in these studies. For other choices of reference, new values of α could be determined by the above procedure.

Absolute values of exchange rates for R1 side chains with either NiEDDA or O_2, calculated as $\alpha\Pi$, are in excellent agreement with the corresponding values determined from SR, regardless of the spectral lineshape (Fig. 7 *B*). This result validates the assumptions underlying the CW power saturation method, and indicates that saturation parameters are indeed valid measures of nitroxide T_{1e} values over a wide dynamic range. This result supports the work of Haas et al. (20) who used spectral simulations to conclude that reliable values of T_{1e} could be extracted from continuous wave saturation curves of nitroxides, even though the lines are inhomogeneously broadened. More recently, Nielsen et al. (30) presented the results of a study that is very similar in intent to that reported here. In that work, the R1 side chain was placed at a number of solvent-exposed sites in phospholipase A2, and Heisenberg exchange with O_2 investigated with both SR and CW power saturation. CW saturation was characterized by a parameter P_2 (rather than $P_{1/2}$ or Π), and fractional changes in P_2 were found to be correlated with fractional changes in $1/T_{1e}$ measured by SR with a correlation coefficient of 0.62. In this study, the correlation between CW-derived and SR-derived values for W_{ex} is much higher, with correlation coefficients of 0.99 and 0.88 for NiEDDA and O_2, respectively. This difference is most likely due to the much smaller dynamic range of accessibilities investigated in the study of Nielsen et al. (30).

Experimental measures of solvent accessibility

In previous work, the R1 side-chain solvent accessibility was measured by the accessibility parameter, Π. This parameter faithfully reflects relative solvent accessibility, and was sufficient to recognize a periodic dependence on sequence that identified secondary structure (5,15). The accessibility factor ρ introduced in this study is on an absolute scale, ranging from 0 to 1, which can be directly compared between laboratories. The accessibility factor has a simple physical meaning, namely the exchange rate constant experienced by the nitroxide in a protein (k_{ex}^P) relative to that experienced by the hypothetical state of the nitroxide in solution that has the same translational diffusion coefficient it had in the protein (k_{ex}*). The hypothetical rate constant is $k_{ex}^* = k_{ex}\,[D_R/D_R + D_N]$, where k_{ex} is the actual exchange rate constant for the nitroxide in solution, here taken to be the reference compound 4-cyano-2,2,5,5-tetramethyl-pryollidine-1-oxyl. The value of ρ depends on the exchange reagent employed, just as the solvent accessibility computed from the crystal structure depends on the radius of the probe used in the calculation (31). As discussed above, NiEDDA is the preferred probe. As shown in Fig. 7 *A*, ρ(NiEDDA) shows a periodic variation with sequence along the 128–135 helix, and varies from essentially 0 to 1, as expected.

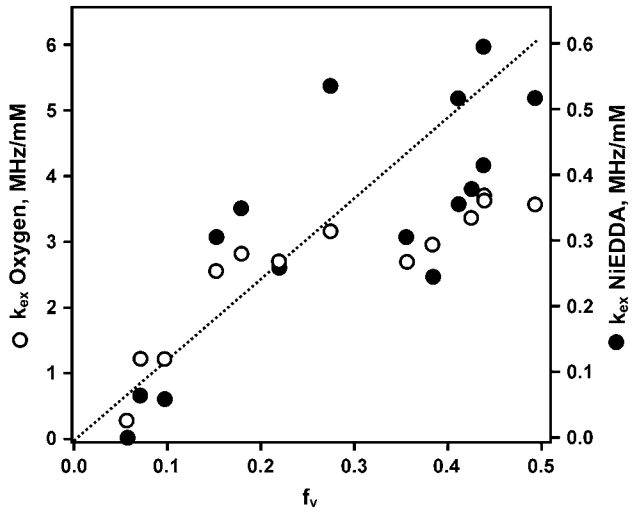

FIGURE 8 Correlation between experimental measures of R1 accessibility (k_{ex}(Oxygen), k_{ex}(NiEDDA)), and the structure-based parameter f_V.

A primary use for an experimental solvent accessibility measure is to permit comparison of solution and crystal structures. For this purpose, it is necessary to have a structure-based measure of ρ(NiEDDA) that can be computed from a known crystal structure. As shown in Fig. 8, the parameter f_V, the factional volume accessibility, is linearly correlated with ρ(NiEDDA), and with $W_{ex}(O_2)$. If this correlation holds for a larger database, it will be possible to compute estimates for f_V for any protein from experimental values of ρ(NiEDDA), and vice versa. This will permit a quantitative comparison of crystal structure data with solution structures determined by nitroxide scanning and associated ρ(NiEDDA) data.

This work was supported by National Institutes of Health (grant EY05216 to W.L.H), Fogarty International Center (TW00456 to W.L.H.), and the Jules Stein Professorship endowment (W.L.H.).

REFERENCES

1. Hubbell, W. L., and C. Altenbach. 1994. Investigation of structure and dynamics in membrane proteins using site-directed spin labeling. *Curr. Opin. Struct. Biol.* 4:566–573.
2. Hubbell, W. L., H. S. Mchaourab, C. Altenbach, and M. A. Lietzow. 1996. Watching proteins move using site-directed spin labeling. *Structure.* 4:779–783.
3. Hubbell, W. L., A. Gross, R. Langen, and M. A. Lietzow. 1998. Recent advances in site-directed spin labeling of proteins. *Curr. Opin. Struct. Biol.* 8:649–656.
4. Hubbell, W. L., D. S. Cafiso, and C. Altenbach. 2000. Identifying conformational changes with site-directed spin labeling. *Nat. Struct. Biol.* 7:735–739.
5. Hubbell, W. L., C. Altenbach, C. M. Hubbell, and H. G. Khorana. 2003. Rhodospin structure, dynamics, and activation. A perspective from crystallography, site-directed spin labeling, sulfhydryl reactivity and disulfide cross-linking. *Adv. Protein Chem.* 63:243–290.
6. Feix, J. B., and C. S. Klug. 1998. Spin labeling: the next millennium. *In* Biological Magnetic Resonance, Vol. 14. L. J. Berliner, editor. Plenum Press, New York, NY. 251–281.
7. Altenbach, C., and W. L. Hubbell. 1998. Site-directed spin labeling: a strategy for determination of structure and dynamics of proteins. *In* Foundations of Modern EPR. G. R. Eaton, S. E. Eaton, and K. M. Salikhov, editors. World Scientific Publishing, Hackensack, NJ. 423–435.
8. Columbus, L., and W. L. Hubbell. 2002. A new spin on protein dynamics. *Trends Biochem. Sci.* 27:288–295.
9. Columbus, L., T. Kalai, J. Jeko, K. Hideg, and W. L. Hubbell. 2001. Molecular motion of spin labeled side chains in alpha-helices: analysis by variation of side chain structure. *Biochemistry.* 40:3828–3846.
10. Altenbach, C., T. Marti, H. G. Khorana, and W. L. Hubbell. 1990. Transmembrane protein structure: spin-labeling of bacteriorhodopsin mutants. *Science.* 248:1088–1092.
11. Rabenstein, M. D., and Y. K. Shin. 1995. Determination of the distance between two spin labels attached to a macromolecule. *Proc. Natl. Acad. Sci. USA.* 92:8239–8243.
12. Hustedt, E. J., and A. H. Beth. 1999. Nitroxide spin-spin interactions: applications to protein structure and dynamics. *Annu. Rev. Biophys. Biomol. Struct.* 28:129–153.
13. Eaton, G. R., S. S. Eaton, and L. J. Berliner. 2000. Distance measurements in biological systems by EPR. *In* Biological Magnetic Resonance, Vol. 19. Kluwer, New York, NY.
14. Altenbach, C., K.-J. Oh, R. Trabanino, K. Hideg, and W. Hubbell. 2001. Estimation of inter-residue distances in spin labeled proteins at physiological temperatures: experimental strategies and practical limitations. *Biochemistry.* 40:15471–15482.
15. Isas, J. M., R. Langen, H. T. Haigler, and W. L. Hubbell. 2002. Structure and dynamics of a helical hairpin and loop region in annexin 12: a site-directed spin labeling study. *Biochemistry.* 41:1464–1473.
16. Molin, Y. N., K. M. Salikhov, and K. I. Zamaraev. 1980. Spin Exchange. Springer-Verlag, New York, NY.
17. Farahbakhsh, Z. T., C. Altenbach, and W. L. Hubbell. 1992. Spin labeled cysteins as sensors for protein lipid interaction and conformation in rhodopsin. *Photochem. Photobiol.* 56:1019–1033.
18. Oh, K. J., C. Altenbach, R. J. Collier, and W. L. Hubbell. 2000. Site-directed spin labeling of proteins. Applications to diphtheria toxin. *Methods Mol. Biol.* 145:147–169.
19. Pyka, J., J. Ilnicki, C. Altenbach, W. L. Hubbell, and W. Froncisz. 2005. Accessibility and dynamics of nitroxide side chains in T4 lysozyme measured by saturation recovery EPR. *Biophys. J.* 89:2059–2068.
20. Haas, D. A., C. Mailer, and B. H. Robinson. 1993. Using nitroxide spin labels. How to obtain T1e from continuous wave electron paramagnetic resonance spectra at all rotational rates. *Biophys. J.* 64:594–604.
21. Mchaourab, H. S., M. A. Lietzow, K. Hideg, and W. L. Hubbell. Motion of spin-labeled side chains in T4 lysozyme. Correlation with protein structure and dynamics. *Biochemistry.* 35:7692–7704.
22. Hubbell, W. L., W. Froncisz, and J. S. Hyde. 1987. Continuous and stopped flow EPR spectrometer based on a loop gap resonator. *Rev. Sci. Instrum.* 58:1879–1886.
23. Smirnov, A. I., R. B. Clarkson, and R. L. Belford. 1996. EPR linewidth (T2) Method to measure oxygen permeability of phospholipid bilayers and its use to study the effect of low ethanol concentrations. *J. Magn. Reson.* 111:149–157.
24. Koradi, R., M. Billeter, and K. Wüthrich. 1996. MOLMOL: a program for display and analysis of macromolecular structures. *J. Mol. Graph.* 14:51–55.
25. Hyde, J. S., and W. K. Subczynski. 1989. Spin label oxymetry. *In* Spin Labeling: Theory and Applications. L. J. Berliner and J. Reuben, editors. Plenum, New York, NY. 399–425.
26. Froncisz, W., and J. S. Hyde. 1982. The loop-gap resonator: a new microwave lumped circuit ESR sample structure. *J. Magn. Reson.* 47:515–521.
27. Wilke, C. R., and P. Chang. 1955. Correlation of diffusion coefficients in dilute solutions. *AIChE J.* 1:264–270.
28. Salikhov, K. M., A. B. Doctorov, Y. N. Molin, and K. I. Zamaraev. 1971. Exchange broadening of EPS lines for solutions of free radicals and transition metal complexes. *J. Magn. Reson.* 5:189–205.
29. Wilhelm, E., R. Battino, and R. J. Wilcock. 1977. Low pressure solubility of gases in liquid water. *Chem. Rev.* 77:219–262.
30. Nielsen, R. D., S. Canaan, J. A. Gladden, M. H. Gelb, C. Mailer, and B. H. Robinson. 2004. Comparing continuous wave progressive saturation EPR and time domain saturation recovery EPR over the entire motional range of nitroxide spin labels. *J. Magn Reson.* 169: 129–163.
31. Lee, B., and F. M. Richards. 1971. The interpretation of protein structures: estimation of static accessibility. *J. Mol. Biol.* 55:379–400.